IOP PUBLISHING EUROPEAN JOURNAL OF PHYSICS

Eur. J. Phys. **30** (2009) 97–108 doi:10.1088/0143-0807/30/1/010

The stability of the catenary shapes for a hanging cable of unspecified length

A Mareno[1] **and L Q English**[2]

[1] Department of Mathematics and Computer Science, Penn State Harrisburg, Middletown, PA 17057, USA
[2] Department of Physics and Astronomy Dickinson College, Carlisle, PA 17013, USA

Received 1 June 2008, in final form 22 August 2008
Published 17 November 2008
Online at stacks.iop.org/EJP/30/97

Abstract

It has long been known that when a cable of specified length is hung between two poles, it takes the shape of a catenary—a hyperbolic cosine function. In this paper, we study a variation of this problem. First, we consider a cable hanging between two poles in which one end of the cable is fixed to one pole; the other end of the cable runs over a pulley, attached to the other pole, and then down to a table. Here, the length of the cable can vary as the pulley rotates. For a specified horizontal distance between the two poles, we vary the height of the fixed cable end. We then determine both experimentally and analytically the stability of the resulting catenary-cable shapes. Interestingly, at certain heights there are two catenaries of different lengths—we use Newtonian mechanics to show that only one of these is stable. Below a certain critical height, no catenary exists and the cable is pulled down to the table. Finally, we explore a related problem in which one end of the cable runs over a pulley, but the other end can now freely move vertically along a pole. These experiments nicely lend themselves as teaching tools in a classroom setting.

1. Introduction

There are a few classic optimization problems which challenged and inspired the greatest mathematicians of the 17th and 18th century and which eventually gave rise to the calculus of variations as a branch of mathematics. Two famous examples are the brachistochrone and the catenary problems [1]. In the catenary problem a flexible cable of specified length is hung between two poles; one must determine the shape of the cable that minimizes the potential energy.

Galileo was the first to formulate this problem in 1638, and he incorrectly speculated that the shape of a hanging cable was a parabola [2, 3]. Subsequently, in the 1690s, the Bernoulli brothers, Huygens and Leibniz, independently found the correct solution, the hyperbolic cosine function. Since then, many variations on this original problem have been studied, some considering non-uniform cables [4], others treating elastic cables [5], networks of cables [6]

and cables with surface tension [3]. All of these studies assume that the length of the cable cannot change in the problem.

Here we describe another variation of the catenary problem and its experimental implementation in which the cable length is allowed to vary. A cable is again hung between two vertical poles. In the first setup, the right end of the cable is fixed to a pole, but on the left side the cable runs through a pulley attached to the other pole. The cable then follows down this pole (on the other side of the pulley) to a reservoir of cable on the table. As the pulley rotates, the length of the cable varies. In a related setup, the boundary condition on the right is changed such that the cable can move freely up and down the right pole.

Several parameters are important here: the heights of the cable at the two ends and the horizontal distance between the two poles. For simplicity, we assume that the horizontal distance between the two poles is fixed and only allow the height of the right end of the cable to vary.

There are essentially two possible cable shapes that minimize the potential energy: the cable will either take the shape of a catenary, or when the cable is 'too' long it will simply lie flat on the table. Which of these two cases is physically realized depends on the height of the right cable end. One can show (see for example exercise 7 in [12]) that there exists a critical height below which the cable begins to unwind. We determine this critical height experimentally as well as analytically by exploring the relationship of the height of the right end of the cable to its length.

In a second setup, we modify the boundary condition on the right side of the cable. We retain the pulley arrangement, but we now keep the right cable end free to move vertically along the pole. The essential parameter in this modified problem is the pulley height as it determines the existence of stable catenaries.

In this paper, we describe the experimental setups of the cable and pulley system outlined above. We have found these experiments to be instructive in a classroom setting as a way to motivate and elucidate the 'calculus of variations' approach to classical mechanics.

Furthermore, we develop a perturbation technique to determine the stability of the catenary using Newtonian mechanics reasoning. At the heart of this technique is a calculation of the cable tension at the pulley for catenaries of various lengths. In contrast to the standard approach using conjugate points from the calculus of variations [7, pp 247–9], we believe that our method is accessible to undergraduate students.

2. Theoretical background and experimental setup

We seek the shape of a uniform cable between two fixed points of suspension that minimizes the potential energy without imposing any constraint on the cable length. To find this shape, the standard procedure is to obtain the Euler–Lagrange equation by setting the first variation of the potential energy functional, $U = \int \mu g y \sqrt{1 + (y')^2}\, \mathrm{d}x$, to zero. Here, μ is the mass per unit length of the cable, g is the gravitational acceleration and y is the height of a cable element. Because the integrand is explicitly independent of x, a first integral of the Euler–Lagrange equation is obtained:

$$\frac{y y'^2}{\sqrt{1 + y'^2}} - y\sqrt{1 + y'^2} = C_1. \tag{1}$$

(See [7, pp 39–40], [9, pp 20–21] and [8] for more information.) After solving for y', one obtains the following integral for x:

$$x = \int \frac{\mathrm{d}y}{\sqrt{\frac{y^2}{C_1^2} - 1}} = C_1 \cosh^{-1} \frac{y}{C_1} + C_2. \tag{2}$$

C_2 is the arbitrary constant of integration. Finally, after inverting the expression for $x(y)$, the general solution is obtained:

$$y(x) = \kappa_1 \cosh\left(\frac{x}{\kappa_1} + \kappa_2\right), \tag{3}$$

where $\kappa_1 = C_1$ and $\kappa_2 = -\frac{C_2}{C_1}$. Here, κ_1 and κ_2 are the two arbitrary constants, and hence equation (3) represents a family of curves.

Experimentally, a straightforward way to obtain a variable length between the suspension points on the poles is to employ a pulley leading to a cable reservoir. The location of the reservoir should be at zero potential energy, i.e. at the level of the table. With this choice, the additional cable is transferred via the pulley from or to zero potential energy, which means that we do not pay a potential energy penalty at the reservoir for lengthening or shortening the catenary. If the cable reservoir were located at the pulley, say, a lengthening of the catenary would always lower the potential energy of the entire system (hanging cable and cable reservoir), and thus no catenary would be stable. In [7, pp 3–5], the author suggests two pulleys and two reservoirs (one on each pole). The mathematical development leading to equation (3) would be the same with two pulleys as with one pulley and the other cable end clamped, since in both setups the length of the chain is not constrained and the potential energies differ only by a constant; experimentally, however, the latter setup is easier to implement and control.

We normalize the horizontal distance between the poles to be one. Furthermore, we restrict ourselves to the case where the height of the left suspension point also equals one. This leaves one free parameter—the height of the right suspension point. Mathematically, we impose the boundary conditions, $y(0) = 1$ and $y(1) = y_1$, which leads to the two constraints (see [5, pp 51–52]):

$$\kappa_1 \cosh(\kappa_2) = 1, \qquad \text{and} \qquad \kappa_1 \cosh\left(\frac{1}{\kappa_1} + \kappa_2\right) = y_1. \tag{4}$$

Using the general formula for the arc-length of a curve,

$$L = \int_0^1 \sqrt{1 + (y')^2}\, \mathrm{d}x, \tag{5}$$

we finally arrive at the following expression for the length of the catenary:

$$L = \kappa_1 \sinh\left(\frac{1}{\kappa_1} + \kappa_2\right) - \kappa_1 \sinh(\kappa_2). \tag{6}$$

The experimental arrangement is depicted in figure 1(a). The cable is a chain of small interlocking metal balls. It is fixed on the right to a vertical position gauge (C), so that the height can be varied continuously over a large range (roughly from 0.1 m to 0.5 m). On the left, the chain is held up to a fixed height of 0.3 m by a Vernier rotary motion sensor [10] which acts as a low-friction pulley (B) after which it travels straight down to the table (A). The horizontal distance between the two suspension points is also 0.3 m. The solid dots appearing in the figure are the result of photo analysis. While the mathematical treatment was done for simplicity in dimensionless units for x and y, the experimental length scale in both the x and y dimensions is 0.3 m. (Thus, 1 is equivalent to 0.3 m).

Enough excess chain rests on the table (representing zero potential energy) so that the suspended chain can freely 'choose' its own optimal length. For instance, when starting with a catenary of insufficient length between the pulley and position gauge, the pulley (rotary motion sensor) rotates clockwise to deliver more chain from the table. Similarly, when too long a catenary is first set up, the pulley can rotate counter clockwise to transfer some chain

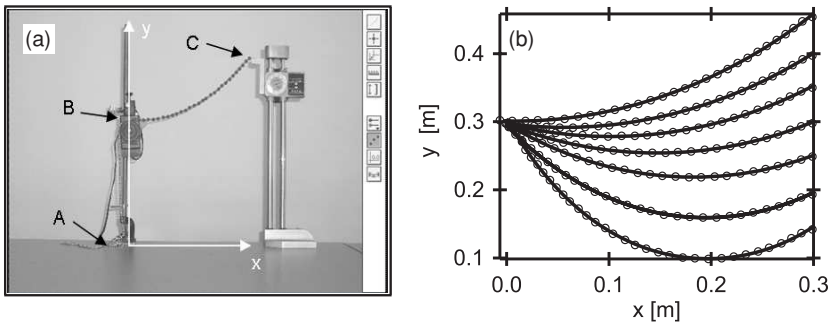

Figure 1. (a) A digital photo taken of the experimental arrangement and imported into Logger Pro for further analysis. (A) the cable reservoir; (B) the pulley-wheel at a fixed height; (C) the other suspension point of the catenary, the height of which is variable. The coordinate system is illustrated in white. The catenary is the graph of the function $y(x)$ between the two suspension points. (b) Photo analysis of seven catenaries is shown by the open circles. Best hyperbolic cosine fits are overlaid.

to the table surface. By monitoring the state of the rotary motion senor (and ensuring that no slippage occurs), changes in catenary length can be tracked.

Data from rotary motion sensor are collected via the Lab Pro interface and Logger Pro software by Vernier [10]. The height of the right suspension point, y_1, can also be monitored continuously by means of a digital linear motion sensor tracking the suspension point (or some point that travels with the suspension point). In this way, the length of the catenary and its right suspension height, y_1, are measured simultaneously.

Another technique employed here is to take digital pictures of catenaries at various suspension heights, y_1. These photos are then imported into Logger Pro, where the shape of the hanging cable can be mapped with great accuracy by clicking on the various interlocking balls (see also [11]). The software then records the coordinates of the points thus selected (relative to a user-defined coordinate system). Figure 1(b) shows the results obtained from seven digital photos taken at values of $y_1 = 0.15$–0.45 m. The circles indicate the measured positions of metal balls along the hanging chain and the solid line indicates the best fit. The fit equation is equation (3) with two independent parameters, κ_1 and κ_2.

3. Results and discussion

3.1. Analytical

On first sight, it may not be obvious why the problem at hand should exhibit a critical height of the right endpoint below which no stable catenary can exist. As a starting point in addressing this question, we seek a relationship between catenary length, L, and height, y_1. Rewriting the expression for L in equation (6) in terms of y_1 yields,

$$L = \pm\kappa_1\sqrt{\cosh^2\left(\frac{1}{\kappa_1}+\kappa_2\right)-1} \mp \kappa_1\sqrt{\cosh^2(\kappa_2)-1}, \tag{7}$$

where the upper sign is used for positive arguments of the hyperbolic cosines and the lower signs for negative ones. Using the first of the two constraints in equation (4), we see that $\cosh(\kappa_2) = \frac{1}{\kappa_1}$. If we substitute this expression for $\frac{1}{\kappa_1}$ into the equation for the second constraint in equation (4), then the left side of this constraint becomes $\kappa_1\cosh(\cosh(\kappa_2)+\kappa_2)$. Since

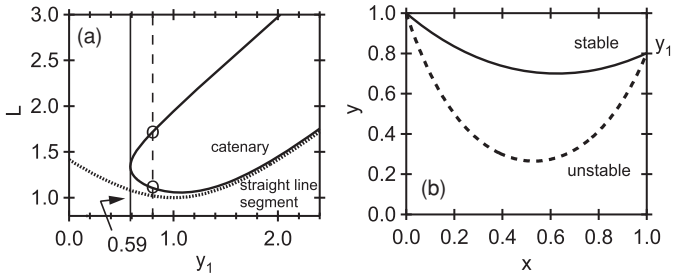

Figure 2. (a) Catenary length versus height as in the previous figure, compared to the length of a straight line segment between the same endpoints (dotted trace). For $0.59 < y_1 \leqslant 2$, the graph shows two catenary solutions of different lengths (see solid line). (b) The two catenaries consistent with $y_1 = 0.8$ are plotted. The longer solution is dynamically unstable.

$\cosh(-x) = \cosh(x) > x$ for any real number x , $\kappa_1^{-1} + \kappa_2$ can never be negative. Therefore, since $\kappa_1^{-1} + \kappa_2 \geqslant 0$, $\sinh\left(\kappa_1^{-1} + \kappa_2\right) \geqslant 0$, and we can drop the first plus–minus symbol in equation (7).

Combining equations (7) and (4) we arrive at the expression

$$L = \sqrt{y_1^2 - \kappa_1^2} \mp \sqrt{1 - \kappa_1^2}. \tag{8}$$

It is important to remember that y_1 depends on κ_1. By the boundary conditions, we have

$$y_1 = \kappa_1 \cosh\left(\frac{1}{\kappa_1} \pm \cosh^{-1}\left(\frac{1}{\kappa_1}\right)\right), \tag{9}$$

where again the lower sign is to be used for negative κ_2.

In figure 2(a), the solid line is a parametric plot of equations (8) and (9), where the parameter κ_1 runs over the interval (0, 1] and both signs are used. κ_1 must stay within this interval in order for y_1 to be positive and L to be real. The graph shows that no catenary solution exists for heights y_1 below about 0.59. We will refer to this value as the critical height. One interesting feature of the parametric plot is that the curve turns around at the critical height, resulting in two catenaries for $0.59 < y_1 \leqslant 2$ (i.e. two values of L for a given y_1). Note that both catenary branches appearing in the figure continue indefinitely to the right beyond the range shown.

The lower and upper circles in the figure correspond, respectively, to the stable and unstable catenaries at a fixed $y_1 = 0.8$, and these two catenaries are then plotted in figure 2(b). These curves were obtained by first determining graphically the two κ_1 values consistent with $y_1 = 0.8$ after plotting equation (9). Upon applying the first boundary condition of equation (4), the corresponding values of κ_2 can be found (both are negative). With these two pairs of constants (κ_1, κ_2) in hand, equation (3) yields the two catenaries of figure 2(b). The upper catenary is stable and the lower one is unstable, as will be demonstrated in the following section.

Let us return to figure 2(a) once more. Note that the figure compares the lengths of the catenary to that of a straight line segment between the same endpoints. As expected, the catenary is always longer than the straight line due to the sagging of the cable. For large heights, the two curves follow one another closely, but as the height is reduced, a gap opens up due to the more pronounced catenary sag (as seen in figure 1(b)). In this regime, the catenary curves up more quickly resulting in a minimum shifted to larger y_1. Note that the left–right symmetry is broken, as the left endpoint height is constrained to be equal to the horizontal distance between the poles (but not the right).

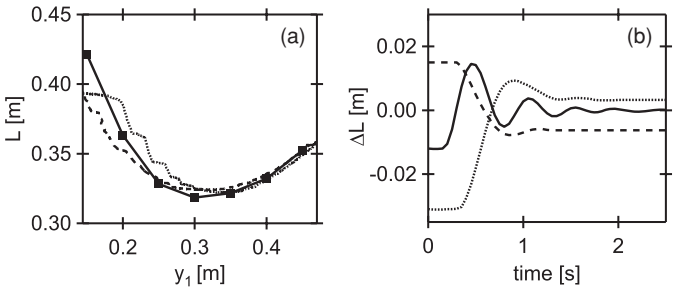

Figure 3. (a) Length of the catenary, L, as a function of suspension height, y_1. The results obtained from photo analysis are superimposed on those obtained from direct measurements. (b) Perturbing the catenary to ascertain its stability: time evolution of the catenary length for $y_1 = 0.35$ m (solid line) and $y_1 = 0.2$ m (dotted and dashed lines).

Thus, the minimum catenary length does not occur at a height of 1, as one might first suspect, but instead at $y_1 = 1.0676$. This number is obtained by substituting equation (9) into equation (8), and then taking the derivative, $\frac{dL}{d\kappa_1}$, which yields

$$\frac{\kappa_1 \cosh(1/\kappa_1 - \cosh^{-1}(1/\kappa_1))}{\sqrt{\kappa_1^2 \cosh^2(1/\kappa_1 - \cosh^{-1}(1/\kappa_1)) - \kappa_1^2}} \times \left\{ \cosh(1/\kappa_1 - \cosh^{-1}(1/\kappa_1)) + \kappa_1 \left[\sinh(1/\kappa_1 - \cosh^{-1}(1/\kappa_1)) \left(-\frac{1}{\kappa_1^2} + \frac{1}{\kappa_1^2 \sqrt{1/\kappa_1^2 - 1}} \right) \right] - 2\kappa_1 \right\} - \frac{\kappa_1}{\sqrt{1 - \kappa_1^2}}. \tag{10}$$

Upon setting this expression to zero and solving numerically for κ_1 we get 0.887, and using equation (9) we finally arrive at $y_1 = 1.0676$. Interestingly, from figure 2(a) we note that for the unstable (longer in figure 2(b)) catenary, the length continues to decrease as the right endpoint is lowered. Here the minimum occurs at the critical height of $y_1 = 0.59$.

3.2. Experimental

Let us now subject some of the analytical predictions in the previous section to the experimental test, remembering that the experimental length scale is 0.3 m which corresponds to 1 in the dimensionless analysis. In the experiment, one quickly finds that when the right suspension point is lowered below a value of around 0.15 m, the chain is quickly pulled down to the table in a run-away fashion. So the existence of a critical height below which the catenary loses stability is easily verified.

Before pinpointing this critical height more precisely, let us first determine the lengths of the measured catenaries depicted in figure 1(b). This can be achieved by first fitting the data points using the hyperbolic cosine model of equation (3). Inserting the resultant best-fit values for κ_1 and κ_2 into equation (6) then yields the experimental lengths. In this way, the lengths of all seven catenaries of figure 2(a) were estimated, and the result is shown by the solid squares in figure 3(a). The graph suggests a minimum catenary length at a height of around 0.3 m (or slightly above it), in agreement with the analytical results.

A more direct method that yields continuous, real-time data was briefly described earlier. Here we directly measure the rotational motion of the pulley as a function of time, while

simultaneously recording the height of the suspension point using a digital motion sensor. The results are depicted by the dotted and dashed lines in figure 3(a). The dashed line represents the data for continuously decreasing heights, starting from 0.45 m, approaching and passing through the critical height of 0.18 m. The dotted line shows the progression back up to 0.45 m.

Comparing these results with those obtained from static photo analysis, we would expect reasonable agreement if the height were varied slowly, so that at each instant the cable had time to settle into the specific catenary which corresponds to the instantaneous boundary conditions. Overall, figure 3(a) indicates reasonable consistency between the two methods. Note, however, that the dotted and dashed lines do not coincide, and their discrepancy is particularly apparent for lower heights. Here we observe qualitatively reproducible hysteretic behaviour. In the analytical section, we showed that the solution given by equation (3) loses its stability at a height of $0.59*(0.3\text{ m}) = 0.18$ m. Thus, for heights between $y_1 = 0.18$ m and 0.2 m, the 'restoring' force on the chain is much reduced and the residual pulley friction becomes more prominent, explaining the lag in length change for both scan directions.

Figure 3(a) demonstrates that in the presence of friction a catenary can be observed in the unstable regime of $y_1 < 0.18$ m. In order to reveal the stability of the various catenaries, we must perturb these solutions. Here we chose to perturb the length of the respective catenaries by turning the pulley-wheel attached to the rotary motion sensor through a fixed angle and letting go. The perturbation angle is then recorded via the rotary motion sensor, and it can be quickly converted to a perturbation length via the radius of the wheel. Figure 3(b) depicts the resultant changes of cable length as a function of time for two different heights, y_1. In each case, the catenary corresponding to a given height was initially perturbed and then allowed to relax. The solid line corresponds to $y_1 = 0.35$ m. The catenary solution is perturbed by reducing the cable length initially. Upon release, the cable quickly returns to the stable catenary via damped oscillations. Repeating this experiment for $y_1 = 0.2$ m, we observe the dotted and dashed lines in figure 3(b). Here, the final state of the cable depends on the sign of the initial perturbation. When the cable length is initially reduced, we end up with a longer catenary than when the cable is initially increased.

At a height of $0.5*(0.3)$ m $= 0.15$ m (not shown in figure 3(b)), a perturbation towards larger lengths always results in the cable being pulled down to the table in a run-away fashion. Thus, experimentally, $0.15 < y_{1,\text{crit}} < 0.2$ m, consistent with the analytical prediction.

Let us compare the results from theory and experiment in more detail. Figure 4 plots catenary length versus height of right endpoint and overlays the experimental and analytical results. The squares, dotted and dashed lines are the experimental results from figure 3 now given in dimensionless units (by dividing by the experimental length scale of 0.3 m). Good agreement is found between the mathematical prediction and the experimental data. Due to slight friction in the experiment, a catenary solution below the critical height can be observed (see the left most data point), though it is unstable against perturbations.

3.3. Newtonian approach to stability

In figure 2(b), we asserted that the upper catenary solution was stable against perturbations whereas the lower one was unstable. In this section, we prove this from a Newtonian point of view. To our knowledge, this line of reasoning has not appeared in the literature. The standard treatment in the literature [7, pp 247–9], [9, pp 106–130] establishing the stability of these catenaries relies on fairly advanced techniques from the calculus of variation (conjugate points).

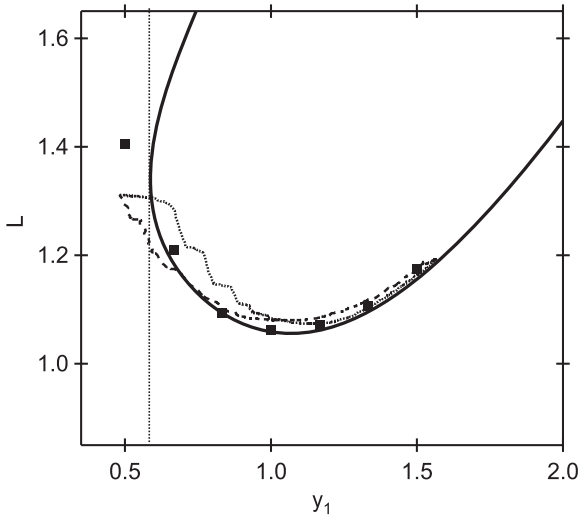

Figure 4. Dependence of catenary length on suspension height (solid line) overlaid on the experimental results.

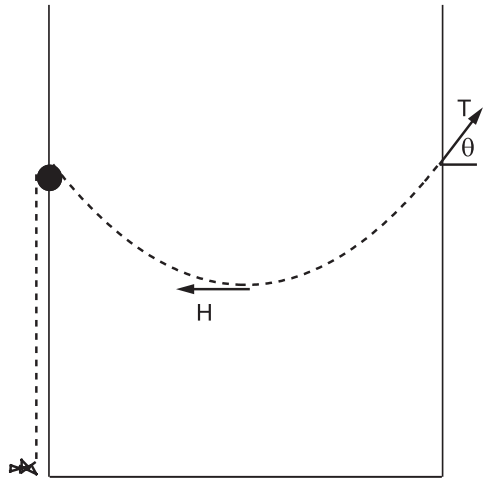

Figure 5. The tension at the cable's lowest point, H, is related to the tension at the right endpoint, T.

In the Newtonian picture, the horizontal component of the tension at any point along the cable has to equal the tension, H, at the bottom of the cable, as depicted in figure 5. This principle comes from the fact that the sum of the forces acting on the cable segment between the cable minimum and the point of interest must be zero. Similarly, the vertical component of the tension must be given by $\mu g s$, where s denotes the arc length. Thus, at the right suspension point of the cable we have (see for example the well-known text [13])

$$\frac{\mu g s}{H} = \tan(\theta) = \left.\frac{\mathrm{d}y}{\mathrm{d}x}\right|_{x=1} = \sinh\left(\frac{1}{\kappa_1} + \kappa_2\right). \tag{11}$$

A simple calculation reveals that the arc length $s = \kappa_1 \sinh\left(\frac{1}{\kappa_1} + \kappa_2\right)$. Using equation (11), and the expression for s, we find that $H = \mu g \kappa_1$. Note that κ_1 is the minimum value for $y(x)$.

Let us now define a perturbation of the catenary solution of equation (3), namely,

$$y(x) = \kappa_1 \cosh\left(\frac{x}{\kappa_1} + \kappa_2\right) + \alpha. \tag{12}$$

This function is still a hyperbolic-cosine, of course, but for $\alpha \neq 0$, equation (12) does not solve the Euler–Lagrange equation (for the unspecified length problem) and thus cannot minimize the potential energy. Therefore, we do not expect these perturbed catenaries to represent stationary chain configurations in our problem. Interestingly, equation (12) is the solution to the classical problem where the length of the cable is fixed *a priori*, and in that problem α represents the Lagrange multiplier. Thus, in a sense, this perturbation analysis samples catenaries that would only be obtained if the pulley wheel were held in place.

Since this perturbed solution is still required to satisfy the boundary conditions, $y(0) = 1$ and $y(1) = y_1$, equation (4) must be modified as follows:

$$\kappa_1 \cosh(\kappa_2) = 1 - \alpha, \qquad \text{and} \qquad \kappa_1 \cosh\left(\frac{1}{\kappa_1} + \kappa_2\right) = y_1 - \alpha. \tag{13}$$

The tension at any point along this perturbed catenary is now found via the following sequence of equalities (see [13]):

$$T(x) = \frac{H}{\cos(\theta)} = H\sqrt{1 + \tan^2(\theta)} = H\sqrt{1 + \sinh^2\left(\frac{x}{\kappa_1} + \kappa_2\right)} = H\left(\frac{y - \alpha}{\kappa_1}\right) = \mu g(y - \alpha). \tag{14}$$

The formula for the length of the perturbed catenary is still given in equation (6). Note that only for $\alpha = 0$ does equation (14) yield a tension at the pulley equal to the weight of chain hanging on the left side of the pulley, and so stationary chain configurations can only arise for $\alpha = 0$.

The basic idea for determining the stability of the catenary solutions to the Euler–Lagrange equation is to plot the length L of the perturbed catenaries versus the tension at the pulley. The tension at this point for the unperturbed catenary (i.e. $\alpha = 0$) is $\mu g y(0) = \mu g$. If the tension at the pulley of the perturbed catenary is less than μg, its length will decrease with time, since the tension on the left side of the pulley, which is always fixed at μg, would then be greater than that on the right side of the pulley, causing chain to be transferred to the reservoir. Similarly, if the tension on the right side of the pulley for the perturbed catenary is greater than μg, then its length will increase. The key is to consider the length in conjunction with the tension for a given perturbed catenary. If the tension is greater than μg and the perturbed catenary is longer than the unperturbed one, we say that the catenary is unstable. If both the tension and the length are smaller than in the unperturbed case, the catenary is again unstable. However, if a larger tension is associated with a smaller length or a smaller tension with a greater length, then the catenary is deemed stable.

Specifically, given values for y_1 and α, we can find κ_1 and κ_2 that satisfy equation (13). Then, equation (8) yields the length and equation (14) yields the tension at the left endpoint. Using this procedure, we calculate L and T for various choices of y_1 and α as summarized in table 1. We conclude that for $y_1 = 1$, the shorter catenary is stable and the longer one is unstable, which corresponds to experiments where the longer catenary solution is never observed. For $y_1 = 0.5$, which is below the critical height, both perturbed catenaries are unstable, as tension on the right side of the pulley must exceed that on the left side of the pulley (see table).

Table 1. The lengths and tensions for both the short and long catenaries computed for two different right endpoints.

$y_1 = 1$		
α	$T/\mu g$	L (short, long)
0	1	(1.054, 1.949)
−0.1	1.1	(1.038, 2.157)
+0.1	0.9	(1.084, 1.723)
$y_1 = 0.5$		
−0.07	1.07	(1.317, 1.459)
−0.1	1.10	(1.339, 1.567)

4. A catenary problem with a natural boundary condition

4.1. Mathematical formulation

In this section, we examine an interesting modification of the previous problem. A brief discussion of this problem can be found in [7, pp 138–9]. Here we only impose one boundary condition, namely that $y(0) = y_0$, and allow the other end of the cable to freely move vertically along the line $x = 1$. Thus $y(1)$ is no longer specified. (Certain restrictions on y_0 will be imposed later.) Using methods from the calculus of variations (see, for example, [9, section 6]), we obtain equation (1) again and the following new boundary condition, which we refer to as a natural boundary condition:

$$\left.\frac{\partial U}{\partial y'}\right|_{x=1} = 0. \tag{15}$$

As before, we arrive at equation (3); now the boundary conditions $y(0) = y_0$ and equation (15) yield

$$\kappa_1 \cosh(\kappa_2) = 1 \qquad \text{and} \qquad y(1)y'(1) = 0. \tag{16}$$

We assume that $y(1) > 0$ since if $y(1) = 0$ the cable simply lies flat on the table. Hence $y(1)y'(1) = 0$ when $y'(1) = 0$. Using equation (3), this condition implies that $\sinh(\frac{1}{\kappa_1} + \kappa_2) = 0$, and so $\kappa_2 = \frac{-1}{\kappa_1}$. Therefore, the general solution to the Euler–Lagrange equation becomes

$$y(x) = \kappa_1 \cosh\left(\frac{x-1}{\kappa_1}\right). \tag{17}$$

We see that $y(1) = \kappa_1$, and the boundary condition $y(0) = y_0$ leads to the equation

$$y_0 = \kappa_1 \cosh\left(\frac{1}{\kappa_1}\right), \tag{18}$$

It is important here to note that there are no values of κ_1 that satisfy equation (18) for $y_0 = 1$, since the hyperbolic cosine is positive and always larger than its argument. However, this equation does have exactly one solution (for κ_1) when $y_0 \cong 1.51$, and two solutions when y_0 is larger than this value. This restriction on the value of y_0 on the boundary leads to an interesting distinction between this free-end boundary problem and our previous problem. For this new problem, we only obtain catenaries when the ratio of the height of the left cable end to the distance between the two poles is approximately 1.51 or larger, but not 1, as in our first problem. Thus, there is no solution for the original pulley height of $y_0 = 1$; only for higher

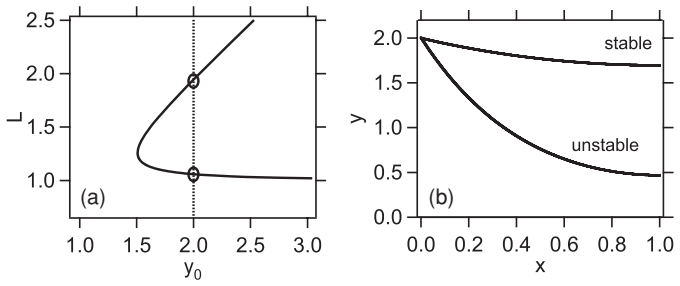

Figure 6. (a) Catenary length versus height of the left endpoint with natural boundary condition on the right. For $y_0 > 1.51$, the graph shows two catenaries of different lengths (see circles). (b) The two catenaries consistent with $y_0 = 2$ are plotted. The longer solution is dynamically unstable.

Table 2. The lengths and tensions for both the short and long catenaries computed for the natural boundary condition on the right.

$y_0 = 2$		
α	$T/\mu g$	L (short, long)
0	2	(1.06, 1.93)
−0.1	2.1	(1.05, 2.05)
+0.1	1.9	(1.07, 1.85)

left endpoints catenaries are found. Finally, using equation (6) and the relation $\kappa_2 = -\frac{1}{\kappa_1}$ we obtain the following simplified expression for the length of the cable:

$$L = \kappa_1 \sinh\left(\frac{1}{\kappa_1}\right). \tag{19}$$

4.2. Analytical and experimental results

Figure 6(a) displays the parametric plot of equations (18) and (19), analogous to figure 2(a). Again we find two catenaries for $y_0 > 1.51$ and no catenaries below this value of y_0. Figure 6(b) depicts the two catenaries for $y_0 = 2$, as indicated by the circles in figure 6(a). Only the shorter catenary is stable, as can be shown using the same Newtonian argument as before. It is straightforward to show that the tension as given in equation (14) remains the same in magnitude under this new boundary condition. Thus, we can apply the previous technique here as well. Table 2 shows the results for a particular $y_0 = 2$. Note that the longer catenary is found to be unstable against both perturbations (i.e. positive and negative α), and the shorter catenary is stable against both perturbations.

Experimentally, this natural boundary condition on the right side of the cable can be realized by using a thin rod at $x = 1$. The chain ends on the right side in a ring that fits over the thin rod and therefore can freely move along the rod. In order to reduce friction, we apply a lubricant to the thin rod. The other aspects of the experiment remain unchanged; the left end of the cable still runs over a pulley with excess cable at the level of the table. It is important to attempt to reduce friction between the chain and the thin rod, otherwise the chain gets stuck and cannot minimize its potential energy. Even at low friction, the chain may have to be perturbed several times until the minimum is reached.

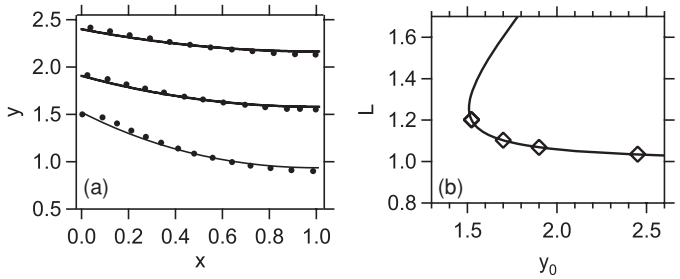

Figure 7. (a) Photo analysis of three catenaries is shown by circles; best hyperbolic cosine fits are overlaid. (b) The lengths of four such catenaries (diamonds) are compared to the theoretical prediction

Figure 7(a) summarizes the experimental data obtained via photo analysis as before. The circles represent the hanging chain and the lines give the best one-parameter fit using equation (17). In figure 7(b), the experimental results for catenary lengths are superimposed on the theoretical curve of figure 6(a) and good agreement is found. At $y_0 = 1.3$ the chain was found to unravel, and no stable catenary was obtained; at $y_0 = 1.4$ the chain did not always spontaneously unravel due to some residual friction.

5. Conclusions

We have examined both analytically and experimentally the variable-length catenary for two boundary conditions; in the first setup, the right end of the catenary was fixed at a particular height, and in the second setup this end was free to move vertically (natural boundary condition). Both cases exhibit critical points for the existence of stable catenaries. In the first case, the height of the right end must be above a certain critical value, and in the second case the height of the left end (i.e., the pulley end) must be above a critical value. As we have described here, both critical points can be discovered experimentally. These experiments are fairly straightforward to carry out, and they nicely illustrate principles from the calculus of variations and from Newtonian mechanics at work.

References

[1] Bliss G A 1925 *Calculus of Variations* (Open Court Publ.) chapters 1 and 4
[2] Goldstine H H 1980 *A History of the Calculus of Variations* (Berlin: Springer)
[3] Behroozi F, Mohazzabi P and McCrickard J P 1994 Remarkable shapes of a catenary under the effect of gravity and surface tension *Am. J. Phys.* **62** 1121–8
[4] Fallis M C 1997 Hanging shapes of nonuniform cables *Am. J. Phys.* **65** 117–22
[5] Antman S S 1979 Multiple equilibrium states of nonlinearly elastic strings *SIAM J. Appl. Math.* **37** 588–604
[6] Pipkin A C 1994 Catenary deformations of inextensible networks *J. Eng. Math.* **28** 401–6
[7] van Brunt B 2004 *The Calculus of Variations* (Berlin: Springer)
[8] Weinstock R 1952 *Calculus of Variations* (New York: McGraw-Hill) pp 30–31
[9] Gelfand I M and Fomin S V 1963 *Calculus of Variations* (Englewood Cliffs, NJ: Prentice-Hall)
[10] *Logger Pro3 Software and Lab Pro Sensor Interface* Vernier Software and Technology
[11] Nedev S 2000 The catenary—an ancient problem on the computer screen *Eur. J. Phys.* **21** 451–57
[12] Goldstein H, Poole C and Safko J 2002 *Classical Mechanics* 3rd edn (Reading, MA: Addison-Wesley) p 65
[13] Jeans J H 1967 *An Elementary Treatise of Theoretical Mechanics* (NewYork: Dover) pp 80–1